

Supporting Information

Analysis of Interdependent Kinetic Controls of Fatty Acid Synthases

Alex Ruppe^a and Jerome M. Fox^{a*}

^aDepartment of Chemical and Biological Engineering, University of Colorado, Boulder,
3415 Colorado Avenue, Boulder, CO, 80303

*To whom correspondence should be addressed. E-mail: jerome.fox@colorado.edu

SI Notes 1-3	S2
Figures S1-S10	S5
Tables S1-S9	S19
Appendix 1	S29
Appendix 2	S34
SI References	S35

SI Notes

SI Note 1. Estimation of Diffusion Limits. We estimated the upper limits of rate constants for intermolecular association (k_{on}) by treating this process as a diffusion-limited reaction between two uniformly reactive spheres. In brief, we used the Stokes-Einstein equation (Eq. S1) to estimate diffusion coefficients (D) and the Smoluchowski expression (Eq. S2) to estimate rate

$$D = \frac{k_B T}{6\pi\eta r} \quad (\text{Eq. S1})$$

$$k_{on} = 4\pi(D_A + D_B)(r_A + r_B) \quad (\text{Eq. S2})$$

constants based on those coefficients.¹ In Eqs. S1-S2, k_B is the Boltzmann constant, T is temperature (300 K), η is the dynamic viscosity of water, r is the radius of a protein or ligand (e.g., small-molecule substrate), and subscripts A and B denote distinct binding partners. We estimated the radii of proteins and ligands from their volumes (i.e., we assumed a spherical volume of $4/3 * \pi r^3$), and we determined those volumes with the following steps: For proteins, we

$$V = \frac{MW}{825} \quad (\text{Eq. S3})$$

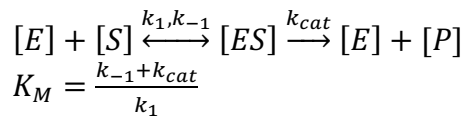
used Eq. S3, where MW is the molecular weight of the protein (Da), and V is its volume (nm³); this empirical relationship assumes a partial molar volume of 0.73 cm³/g, a reasonable estimate for a wide range of proteins.^{2,3} For ligands, we used the PhysChem module of the ACD/Labs property prediction service (www.chemspider.com). Estimates of k_{on} , thus determined, were similar between different varieties of protein-protein or protein-ligand interactions (i.e., within each class of interaction, the standard deviation of k_{on} was ~ 2%), so we used average values of $6.29 \times 10^2 \mu\text{M}^{-1} \text{ s}^{-1}$ for all protein-protein interactions and $1.65 \times 10^3 \mu\text{M}^{-1} \text{ s}^{-1}$ for all protein-ligand interactions.

SI Note 2. Titration Experiments with FabD and FabG. We validated our kinetic model by comparing predicted trends in initial rates of fatty acid synthesis to previously reported measurements of those rates. For this comparison, we used titration data for ACP, FabH, FabZ, FabI, FabF, and TesA (Figures 2-4) because these components have been observed to enhance or inhibit fatty acid synthesis.⁴ We did not examine similar data for FabD and FabG, in turn, because the kinetic contributions of these enzymes are controversial and, thus, represent poor observables for model validation. (For example, the results of an *in vitro* analysis suggest that FAS activity is insensitive to changes in the concentrations of FabD and FabG,⁴ but findings from an *in vivo* study show that overexpression of FabD can increase fatty acid production in *E. coli*).⁵ Nonetheless, to complete our titration studies, we examined the contribution of FabD and FabG to FAS activity (Figure S5). Intriguingly, initial rates were insensitive to changes in the concentrations of FabG (above very low concentrations) but showed a pronounced sensitivity to FabD—a result consistent with both our sensitivity analysis (Figure 9) and the observed influence of carbon flux, which is gated by FabD, on total production (Figure 5).

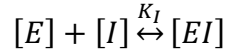
SI Note 3. The Influence of Measurement Time and Substrate Concentration. For much of our study, we examine total production and product distribution at 12.5 minutes. To determine how this choice of measurement time affected observed trends in FAS outputs, we repeated the analyses reported in Figures 6 and 7B at 2.5 and 25 minutes. Interestingly, total production differed by ~fivefold between these time points, but general trends in production and chain length remained similar between them (Figures S6, and S8). The consistent trends exhibited at 2.5, 12.5, and 25 minutes suggest that differences in outputs of various FAS compositions—at least within the 2.5- to 25-minute span of times—result from differences in the steady-state kinetics of fatty acid production, not from differences in production at early or late time points (i.e., discrepancies that would grow or diminish with sample time).

Substrate concentrations represent another possible source of bias in our kinetic analysis. For our study, we chose substrate concentrations (0.5 mM for malonyl-CoA and 0.5 mM for acetyl-CoA) based on physiologically relevant FAS compositions examined by Khosla and colleagues.⁴ To determine how the choice of concentrations affected observed trends in FAS outputs, we repeated the analysis of Figure 6 at different concentrations of malonyl-CoA and acetyl-CoA (Figure S7). To our satisfaction, trends in production and chain length remained similar across different substrate concentrations (within a reasonable range of concentrations).

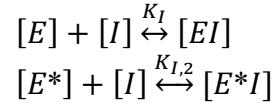
Michaelis-Menten Kinetics:



Competitive Inhibition:



Mixed Inhibition:



Activation⁶:

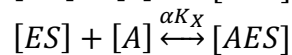
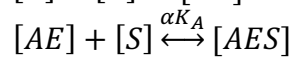
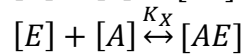
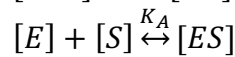
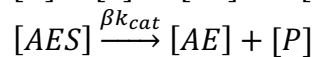


Figure S1. Kinetic models. We reference these models in the main text and supporting information.

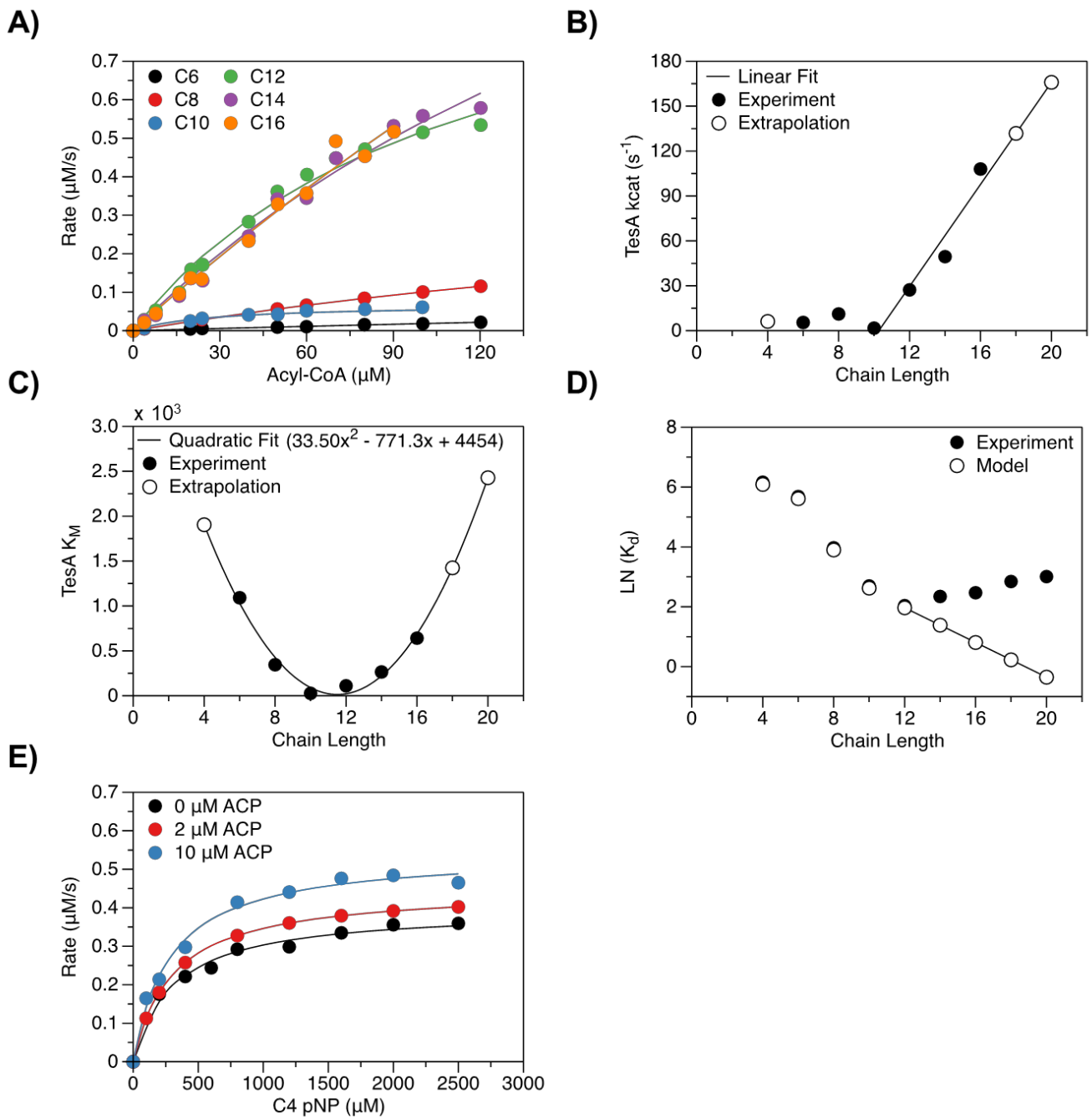


Figure S2. Analysis of TesA kinetics. (A) We estimated values of k_{cat} and K_M for TesA-catalyzed hydrolysis of acyl-CoAs by fitting a Michaelis-Menten model (solid lines) to previously reported kinetic data (filled circles; Table S2).⁷ (B) Values of k_{cat} determined from fits described in A (filled circles) or an extrapolation of those fits (open circles). We estimated values of k_{cat} for C_{18} and C_{20} acyl-CoAs by extrapolating the linear trend exhibited by values of k_{cat} for

C_{10} - C_{16} acyl-CoAs ($r^2 = 0.943$); we estimated a k_{cat} for C_4 acyl-CoA, in turn, by averaging the k_{cat} 's of C_6 - C_{10} acyl-CoAs. (C) Values of K_M determined from fits described in A (filled circles) or an extrapolation of those fits (open circles). Values of K_M for C_6 - C_{16} acyl-CoAs fit well to a second-order polynomial ($r^2 = 0.97$), so we used this polynomial to estimate values of K_M for C_4 , C_{18} , and C_{20} acyl-CoAs. (D) Values of $\ln(K_d)$ determined from K_M 's described in C (filled circles) or an optimization of our kinetic model (open circles). For C_4 - C_{12} acyl-CoAs, experimentally derived and model-based estimates of $\ln(K_d)$ overlap with one another. (E) Initial rates of TesA-catalyzed hydrolysis of p-nitrophenyl-butyrate (pNP4) in the presence of increasing concentrations of ACP. Lines represent fits to an activation model (Table S3), which allowed us to estimate a K_d for the ACP-TesA complex (i.e., K_x in Figure S1).

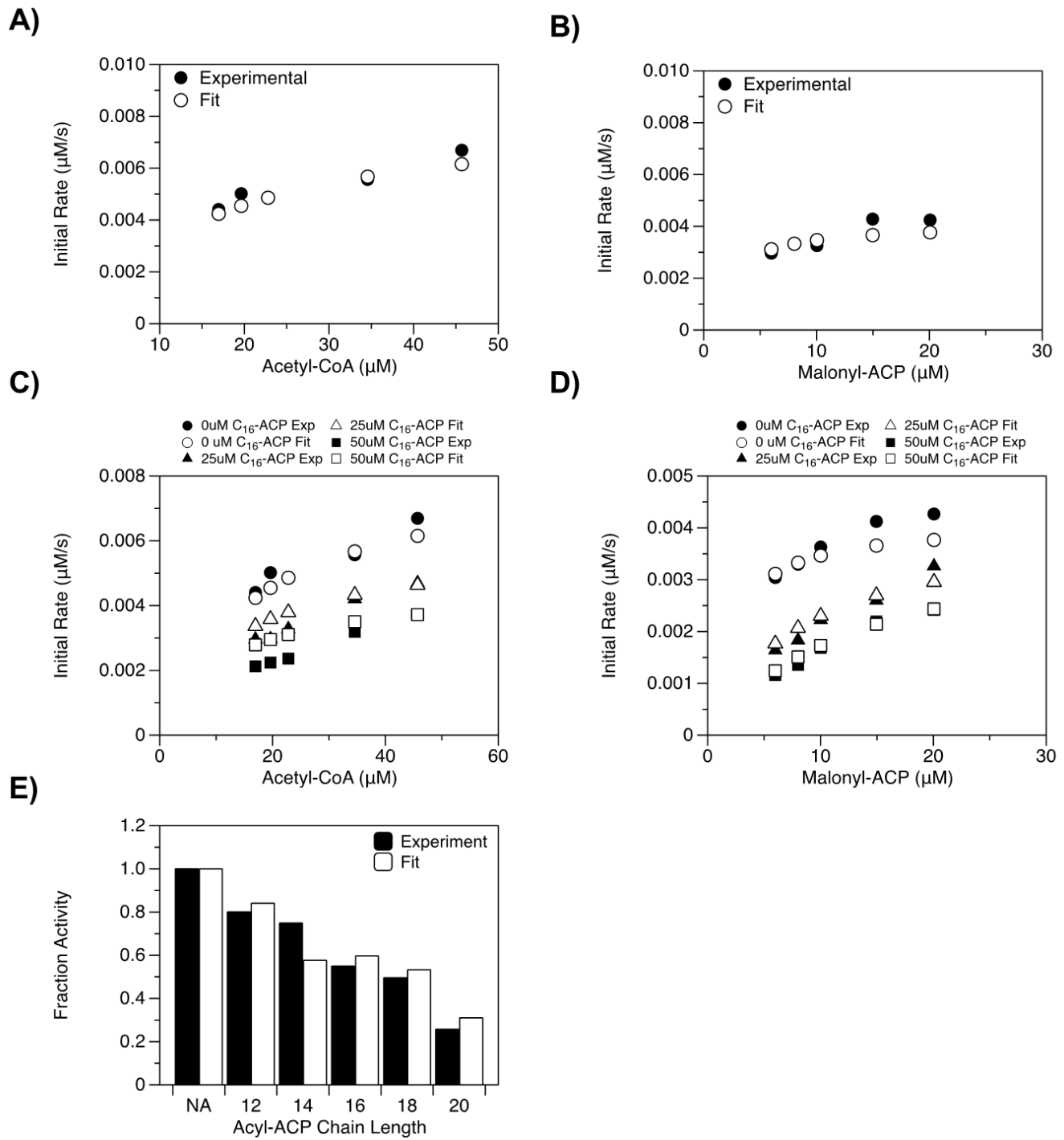


Figure S3. Analysis of FabH inhibition. We modeled inhibition of FabH by acyl-ACPs by using previously reported kinetic measurements.⁸ (A-B) To begin, we fit a kinetic model of FabH-catalyzed condensation of acetyl-CoA and malonyl-CoA (lines 3 and 4 in Table 1, open circles)

to initial rates of condensation (filled circles) determined at different concentrations of (A) acetyl-CoA and (B) malonyl-CoA. (C-D) We fit a model for competitive inhibition to initial rates determined in the presence of varying concentrations of C₁₆-ACP and (C) acetyl-CoA or (D) malonyl-CoA; that is, we fit only K_{I,1} and K_{I,2} as defined in Table S1 and retained the kinetic parameters determined in A-B. (E) We estimated length-specific values of K_{I,1} and K_{I,2}, in turn, by fitting them to measurements of initial rates made in the presence of acyl-ACPs of different lengths (“NA” indicates an initial rate determined in the absence of acyl-ACPs). Table S4 shows estimates of k_{off} and k_{on} based on our initial fit to this data, and Table S7 shows the final inhibition parameters of our optimized model.

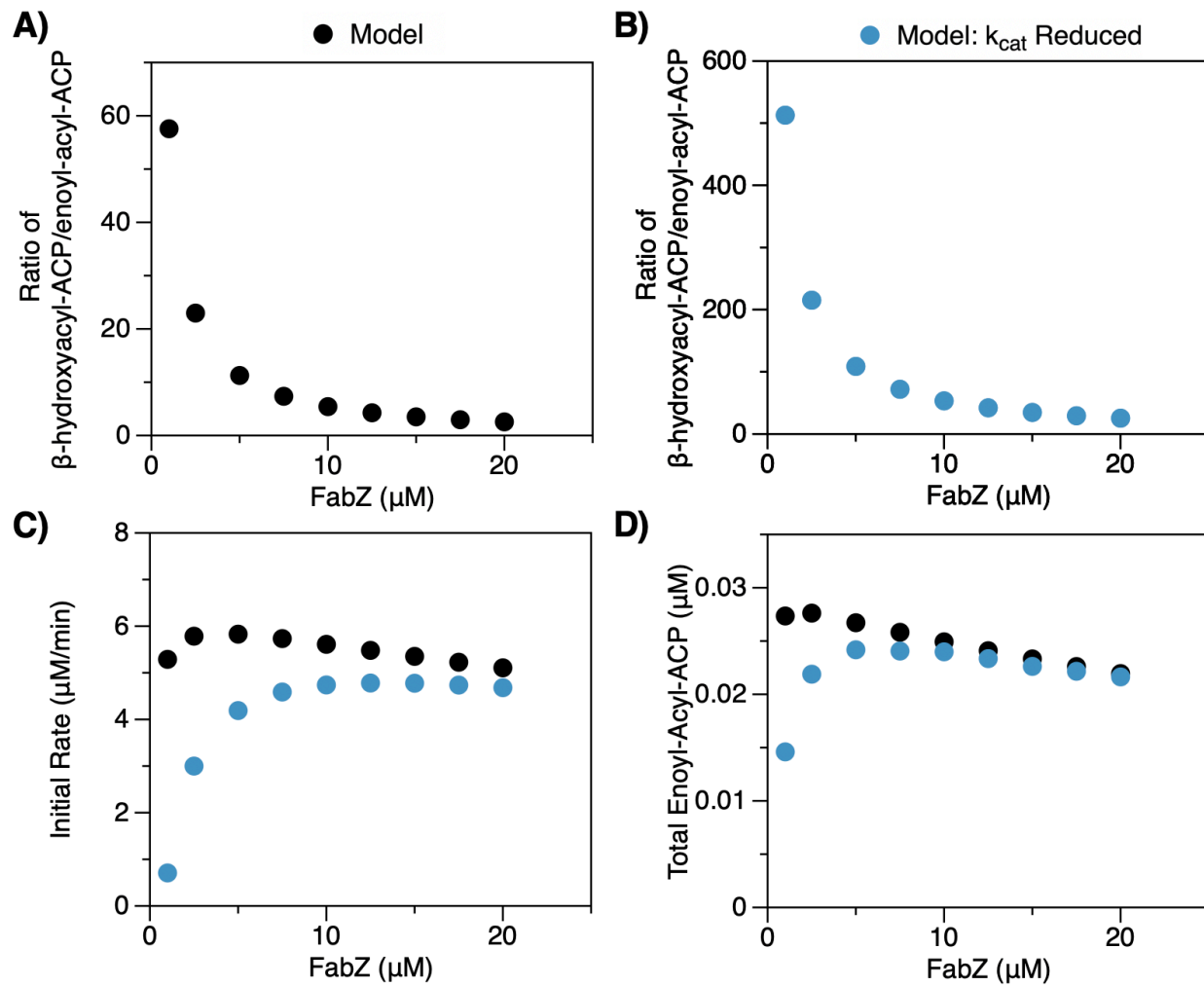


Figure S4. Analysis of FabZ kinetics. (A-B) The ratio of β -hydroxyacyl-ACP to enoyl-acyl-ACP generated by modeled FASs (1 μM of each Fab, 10 μM TesA, 10 μM holo-ACP, 1 mM NADPH, 1 mM NADH, 0.5 mM malonyl-CoA, and 0.5 mM acetyl-CoA, 12.5 min) with varying concentrations of FabZ. In both (A) the base model and (B) the model in which we reduced the k_{cat} of FabZ by tenfold, this ratio is high, relative to the ratio expected at equilibrium (~4:1).⁹ (C) FabZ enhances rates of fatty acid synthesis until (D) concentrations of enoyl-acyl-ACP cease to increase.

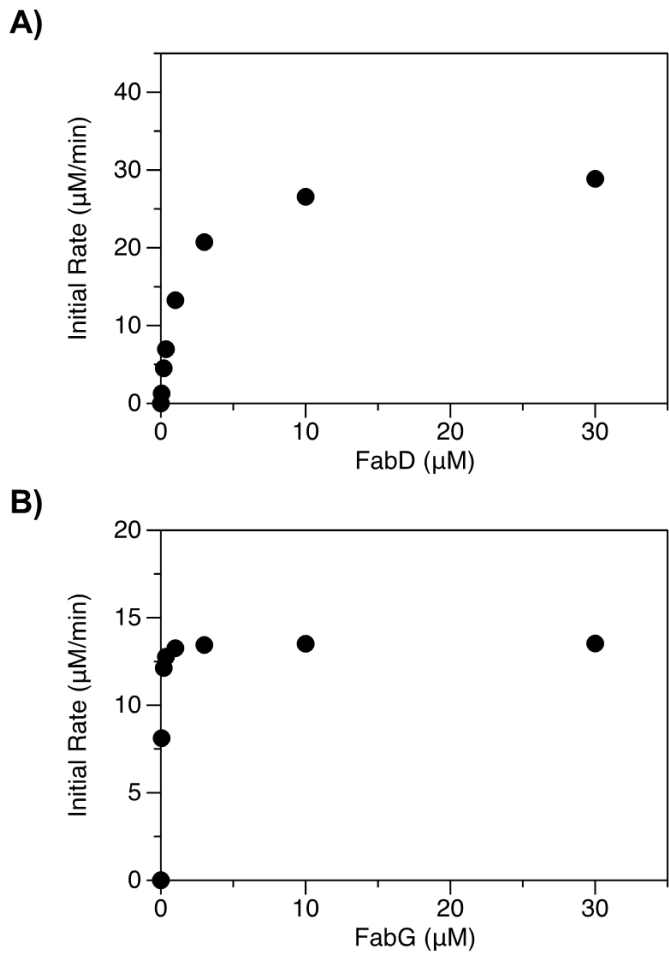


Figure S5. Titration of FabD and FabG. (A-B) Initial rates of fatty acid synthesis exhibited by reconstituted FASs (1 μ M of each Fab, 10 μ M TesA, 10 μ M holo-ACP, 1 mM NADPH, 1mM NADH, 0.5 mM malonyl-CoA, and 0.5 mM acetyl-CoA, 2.5 min) with varying concentrations of (A) FabD and (B) FabG. Rates are highly sensitive to FabD, but not FabG, a result consistent with our sensitivity analysis (Figure 9).

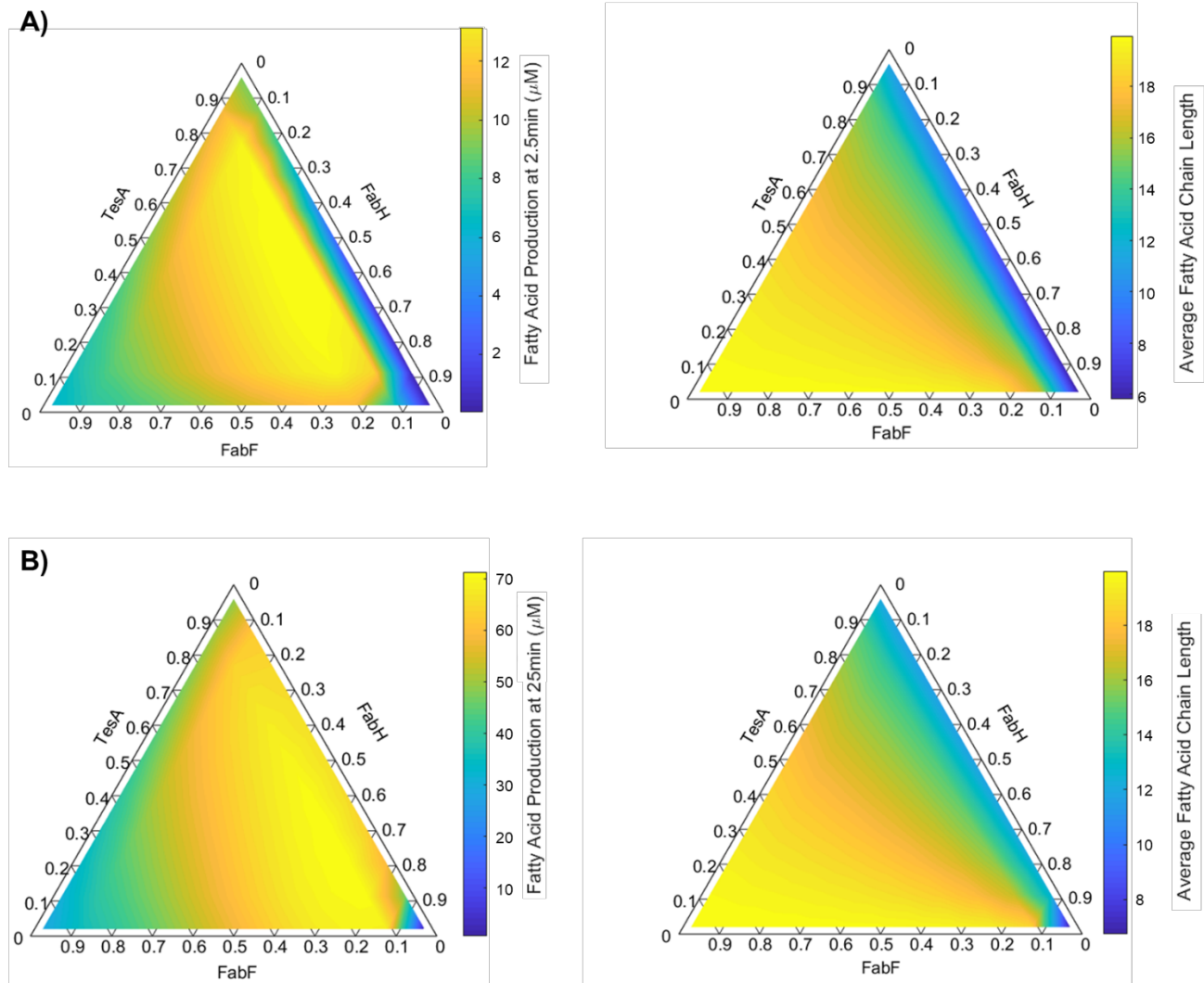


Figure S6. The influence of measurement time on compositional effects. (A-B) Ternary diagrams show total production (left) and average length (right) of fatty acids generated by modeled FASs (1 μM of each Fab, 10 μM holo-ACP, 1 mM NADPH, 1 mM NADH, 0.5 mM malonyl-CoA, 0.5 mM acetyl-CoA) in which ratios of FabH, FabF, and TesA vary (i.e., $[\text{FabH}] + [\text{FabF}] + [\text{TesA}] = 12 \mu\text{M}$). (A) 2.5 minutes and (B) 25 minutes. Compositions with low concentrations of FabF show disproportionately low fatty acid production at 2.5 minutes (i.e., in the diagram on the upper left, the lower right is blue); general trends across the diagrams, however, remain similar between measurement times and, thus, appear to reflect differences in the steady-state kinetics of fatty acid production between compositions.

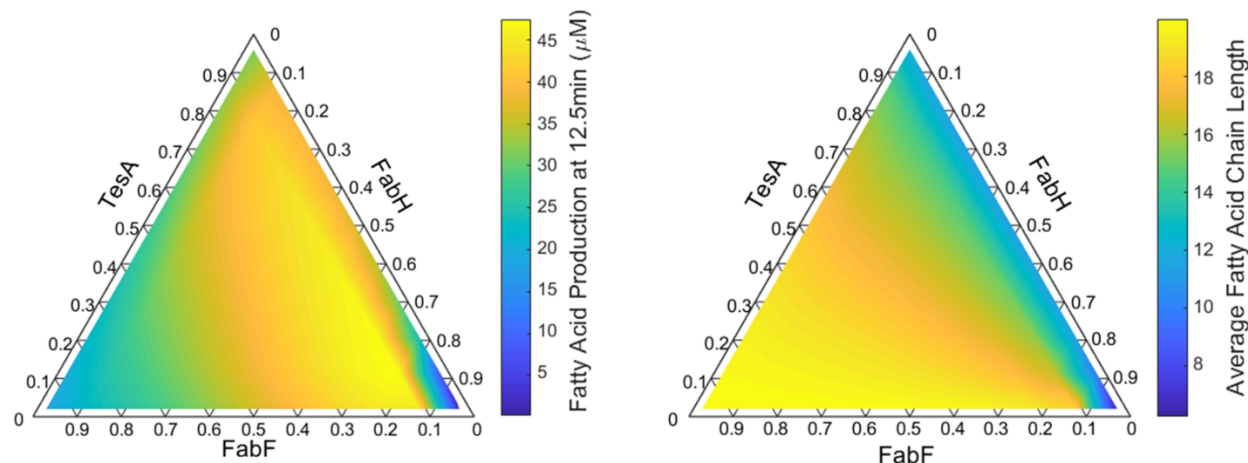
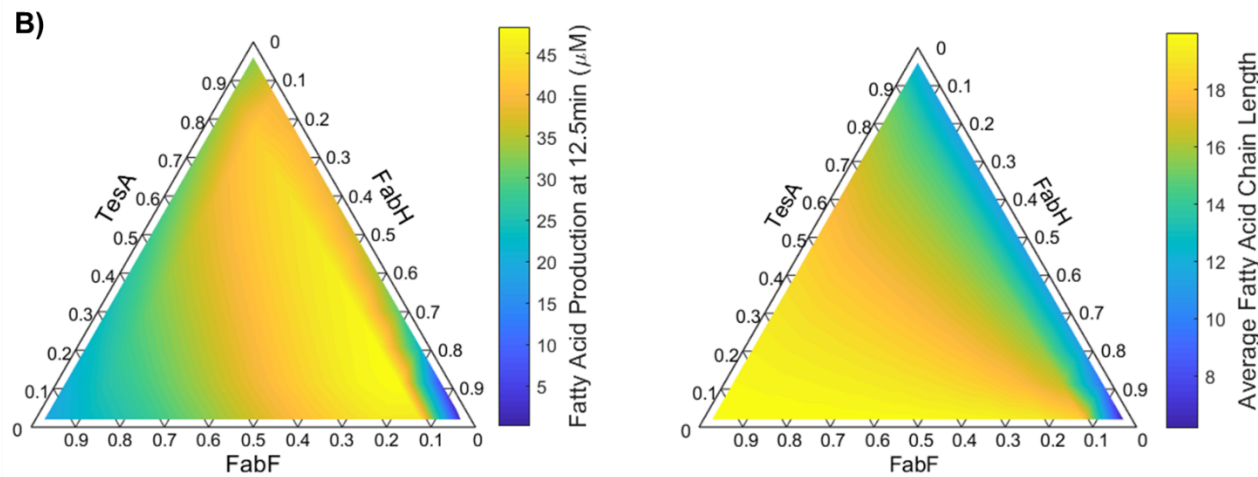
A)**B)**

Figure S7. The influence of substrate concentration on compositional effects. (A-B) Ternary diagrams show the total production (left) and average length (right) of fatty acids generated by modeled FASs (1 μM of each Fab, 10 μM holo-ACP, 1 mM NADPH, and 1mM NADH at 12.5 min) in which ratios of FabH, FabF, and TesA vary (i.e., $[\text{FabH}]+[\text{FabF}]+[\text{TesA}] = 12 \mu\text{M}$). Patterns are similar for (A) 500 μM of malonyl CoA and 500 μM acetyl-CoA and (B) 2500 μM malonyl CoA and 2500 μM acetyl-CoA; they, thus, appear to be independent of substrate concentration (within a reasonable range of concentrations).

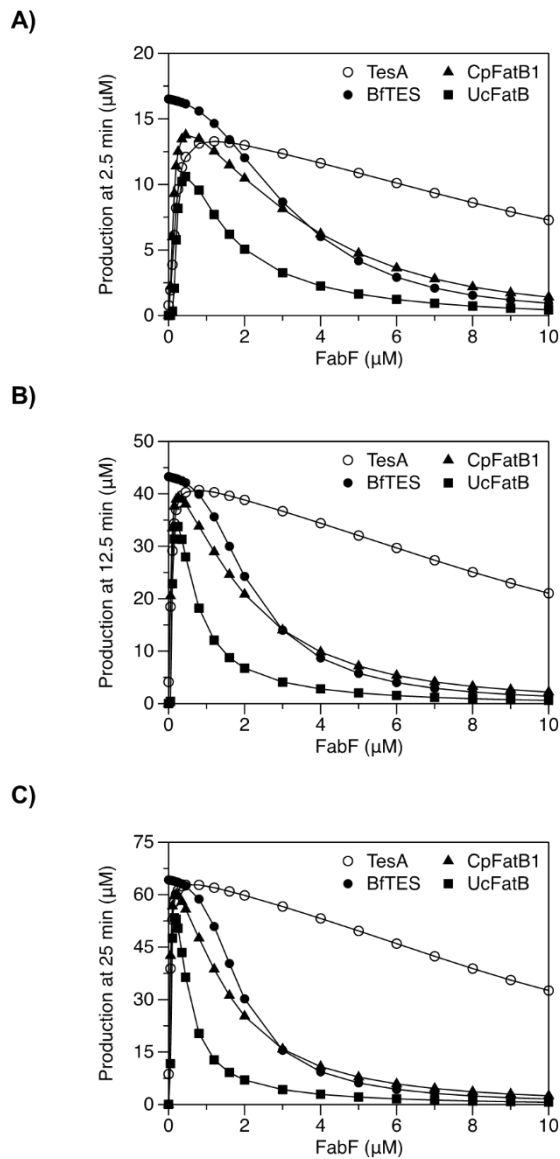


Figure S8. The influence measurement time on the thioesterase-dependence of FabF concentration. (A-C) Total fatty acid production generated by modeled FASs (1 μM of each Fab, 10 μM TesA, 10 μM holo-ACP, 1 mM NADPH, 1 mM NADH, 0.5 mM malonyl-CoA, 0.5 mM acetyl-CoA) with varying concentrations of FabF at (A) 2.5, (B) 12.5, and (C) 25 minutes. The consistency of trends across time points suggests that these trends result from differences in the steady-state kinetics of fatty acid production, not from differences in production at early or late time points (i.e., discrepancies that should change with sample time).

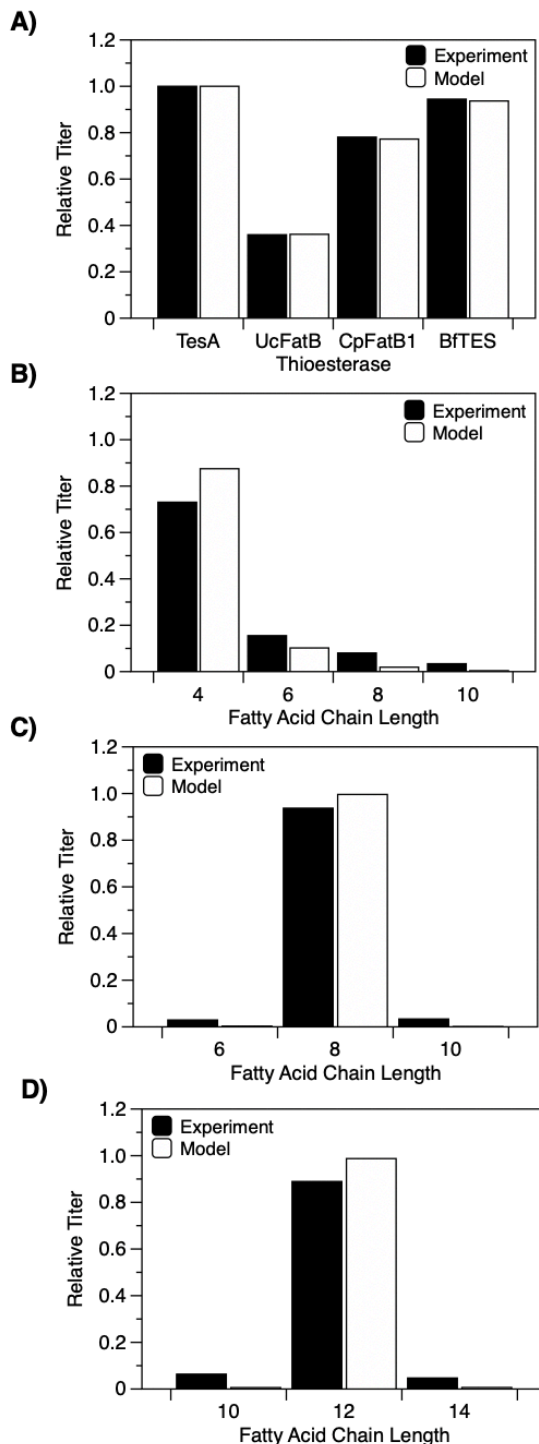


Figure S9. Analysis of plant-derived thioesterases. (A) Relative titers (i.e., palmitic acid equivalents) of fatty acids generated by strains of *E. coli* containing different thioesterases,^{10,11} we normalized each titer by the titer of the TesA-containing strain. (B-D) Approximate product distributions generated by strains containing (B) BfTES, (C) CpFatB1, and (D) UcFatB; we

normalized each plot by total production.¹¹ We note: The reported product profiles of all strains¹¹ showed low concentrations of off-target fatty acids (e.g., C₁₀, C₁₂, C₁₄, C₁₆, and C₁₈ for BfTES); however, these low concentrations—and their consistency across different thioesterase-containing strains—suggest that they arise from nonspecific background activities. Accordingly, panels B-D show only products close in length to the thioesterase-specific products (i.e., those most likely to be “true” off-target products of the thioesterases under study). For A-D, we prepared the model profiles by optimizing thioesterase-specific compositions to A (see main text); Table S8 shows the final optimized kinetic parameters for plant-derived thioesterases.

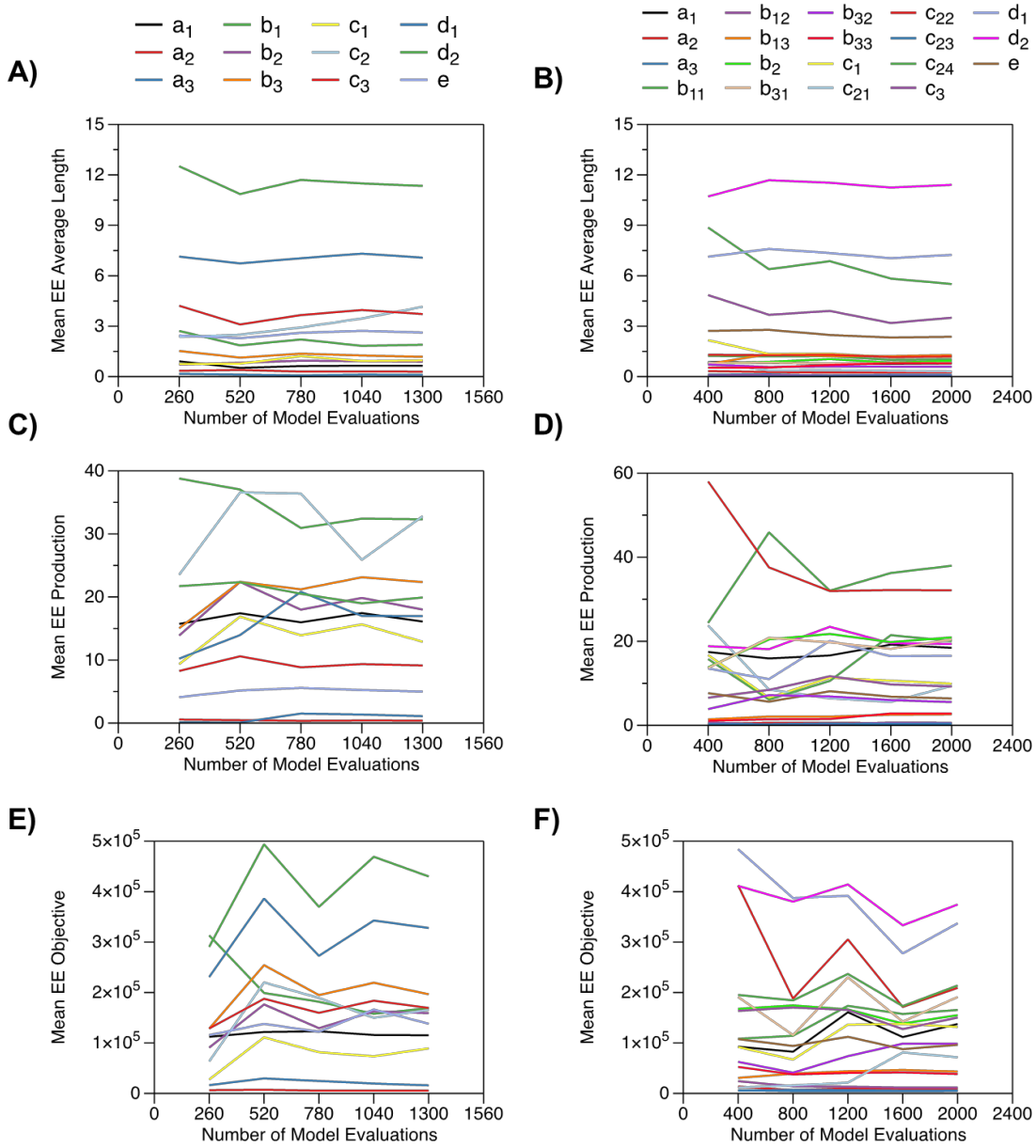
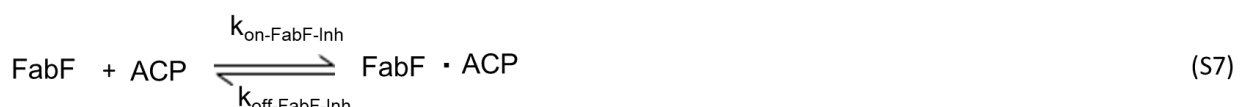
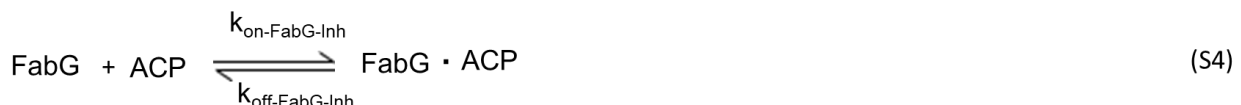
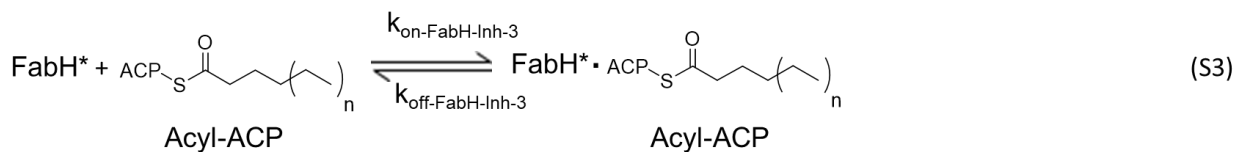
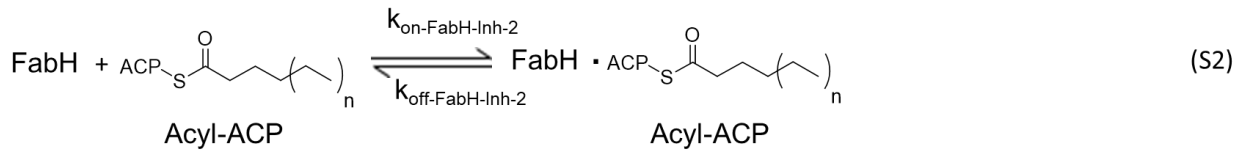


Figure S10. Analysis of the convergence of elementary effects (EE). (A-F) We ensured convergence of elementary effects by examining estimates determined from different numbers of model evaluations. In brief, (i) we determined the total number of evaluations (N) necessary to carry out sensitivity analyses of the kinetic model (A, C, and E) and the expanded version of that model (B, D, and F) by multiplying the number of trajectories (r , the number of initial points used to calculate the elementary effect) by the number of model variables (M) plus one (i.e., $N =$

$r^*[M+1] = 100*[12+1]$ or $100*[19+1]$). (ii) We estimated the mean elementary effect for each trajectory (i.e., collection of 100 points). (iii) We averaged the mean elementary effects estimated from different subsets of trajectories chosen at random among all subsets (e.g., 20, 40, 60, 80, 100 trajectories for each model). The figures show the results of our sensitivity analysis of three objectives: (A-B) average length, (C-D) total production, and (E-F) a fitting objective sensitive to both length and total production (i.e., Obj_A , the product of the sums of squared errors between predicted and measured trends in Figures 2A and 2B; see Materials and Methods).

Table S1. Mechanisms of Inhibition.



*ACP refers to holo-ACP.

^{**}FabD*, FabH*, and FabF* represent refer to acyl-enzyme intermediates.

**In our analysis of FabH inhibition (Fig. S3), we defined values of K_{11} and K_{12} (Fig. S1) as follows:

In our analysis of FabH inhibition (Fig. S3), we defined value $K_{I,1} = k_{off-FabH-Inh2}/k_{on-FabH-Inh2}$ and $K_{I,2} = k_{off-FabH-Inh-3}/k_{on-FabH-Inh-3}$.

Table S2. Kinetic Parameters for TesA-Catalyzed Hydrolysis of Acyl-CoAs.

Enzyme	Substrate	k_{cat} (1/s)	K_M (μM)	K_d (μM)
TesA	C ₆ -CoA	5.50	1090	294
TesA	C ₈ -CoA	11.1	345	53.0
TesA	C ₁₀ -CoA	1.71	27.3	14.8
TesA	C ₁₂ -CoA	27.3	111	7.15
TesA	C ₁₄ -CoA	49.5	265	4.0
TesA	C ₁₆ -CoA	108	642	2.25

*C_i-CoA refers to acyl-CoA with *i* carbons in its acyl chain.

*Parameters determined from the fit described in Fig. S2A.

Table S3. Kinetic Parameters for ACP-Mediated Inhibition of TesA.

Parameter	Value	Units
K_A	308.6	μM
K_X	8.96	μM
α	0.862	unitless
β	1.654	unitless
k_{cat}	3.97	s^{-1}

*Parameters determined from the fit described in Figure S2E.

Table S4. Estimates of Kinetic Parameters.

Enzyme	Parameter	Model Label	Value	Units	Source
FabD	$K_{M\text{-}mCoA}$	N/A	6.0 E1	μM	¹²
FabD	$k_{on\text{-}mCoA}$	$k2_1f$	1.33 E-3	$\mu M^{-1} s^{-1}$	Estimate from K_m^*
FabD	$k_{off\text{-}mCoA}$	$k2_1r$	8.0 E-2	s^{-1}	^{13**}
FabD	$k_{f\text{-}FabD^*}$	$k2_2f$	1.58 E3	s^{-1}	Estimate from FabD k_{cat}^{***}
FabD	$k_{r\text{-}FabD^*}$	$k2_2r$	1.0 E-2	$\mu M^{-1} s^{-1}$	^{****}
FabD	$K_{M\text{-}ACP}$	N/A	3.51 E-1	mM	¹⁴
FabD	$k_{on\text{-}ACP}$	$k2_3f$	5.02 E-2	$\mu M^{-1} s^{-1}$	¹⁵
FabD	$k_{off\text{-}ACP}$	$k2_3r$	2.17 E-2	s^{-1}	¹⁵
FabD	$k_{ffFabD^*\text{-}ACP}$	$k2_4f$	1.58 E3	s^{-1}	Estimate from FabD k_{cat}^{***}
FabD	$k_{rFabD^*\text{-}ACP}$	$k2_4r$	1.0 E-2	$\mu M^{-1} s^{-1}$	^{****}
FabD	k_{cat}	$kcat2$	1.58 E3	s^{-1}	¹⁴
FabH	$K_{M\text{-}aCoA}$	N/A	4.0 E1	μM	¹⁶
FabH	$k_{on\text{-}aCoA}$	$k3_1f$	2.0 E-3	$\mu M^{-1} s^{-1}$	Estimate from K_m^*
FabH	$k_{off\text{-}aCoA}$	$k3_1r$	8.0 E-2	s^{-1}	^{13**}
FabH	$k_{f\text{-}FabH^*}$	$k3_2f$	1.58 E3	s^{-1}	Used $k_{f\text{-}FabD^*}$ from FabD
FabH	$k_{r\text{-}FabH^*}$	$k3_2r$	1.0 E-2	$\mu M^{-1} s^{-1}$	^{****}
FabH	$K_{M\text{-}mACP}$	N/A	5.0 E0	μM	¹⁶
FabH	$k_{on\text{-}mACP}$	$k3_3f$	5.02 E-2	$\mu M^{-1} s^{-1}$	Used $k_{on\text{-}ACP}$ from FabD
FabH	$k_{off\text{-}mACP}$	$k3_3r$	2.17 E-2	s^{-1}	Used $k_{off\text{-}ACP}$ from FabD
FabH	$k_{on\text{-}ACP}$	$k_{on\text{-}I-1}$	2.41E-05	$\mu M^{-1} s^{-1}$	^{8, this study}
FabH	$k_{off\text{-}ACP}$	$k_{off\text{-}I-1}$	2.17E-02	s^{-1}	^{8, this study}
FabH	$k_{on\text{-}C(4-20)ACP}$	$k_{on\text{-}I-2, C(4-20)}$	3.09E-1	$\mu M^{-1} s^{-1}$	^{8, this study}
FabH	$k_{off\text{-}C(4-12)ACP}$	$k_{off\text{-}I-2, C(4-12)}$	1.34E3	s^{-1}	^{8, this study}
FabH	$k_{off\text{-}C14ACP}$	$k_{off\text{-}I-2, C14}$	2.55E2	s^{-1}	^{8, this study}
FabH	$k_{off\text{-}C16ACP}$	$k_{off\text{-}I-2, C16}$	2.99E2	s^{-1}	^{8, this study}
FabH	$k_{off\text{-}C18ACP}$	$k_{off\text{-}I-2, C18}$	7.77E1	s^{-1}	^{8, this study}
FabH	$k_{off\text{-}C20ACP}$	$k_{off\text{-}I-2, C20}$	3.98E1	s^{-1}	^{8, this study}
FabH	$k_{on\text{-}C(4-20)ACP-FabH^*}$	$k_{on\text{-}I-3, C(4-20)}$	1.55E0	$\mu M^{-1} s^{-1}$	^{8, this study}
FabH	$k_{off\text{-}C(4-12)ACP-FabH^*}$	$k_{off\text{-}I-3, C(4-12)}$	3.67E1	s^{-1}	^{8, this study}
FabH	$k_{off\text{-}C14ACP-FabH^*}$	$k_{off\text{-}I-3, C14}$	4.67E1	s^{-1}	^{8, this study}
FabH	$k_{off\text{-}C16ACP-FabH^*}$	$k_{off\text{-}I-3, C16}$	1.17E1	s^{-1}	^{8, this study}
FabH	$k_{off\text{-}C18ACP-FabH^*}$	$k_{off\text{-}I-3, C18}$	1.32E1	s^{-1}	^{8, this study}
FabH	$k_{off\text{-}C20ACP-FabH^*}$	$k_{off\text{-}I-3, C20}$	3.89E0	s^{-1}	^{8, this study}
FabH	k_{cat}	$kcat3$	3.13 E0	s^{-1}	¹⁷
FabG	$K_{M\text{-}NADPH}$	N/A	1.0 E-2	mM	¹⁸
FabG	$k_{on\text{-}NADPH}$	$k4_1f$	1.54 E-3	$\mu M^{-1} s^{-1}$	Used $k_{on\text{-}NADH}$ from FabI
FabG	$k_{off\text{-}NADPH}$	$k4_1r$	7.93 E-2	s^{-1}	Used $k_{off\text{-}NADH}$ from FabI
FabG	$K_{M\text{-}\beta kaACP}$	N/A	1.70 E-2	mM	¹⁹
FabG	$k_{on\text{-}\beta kaACP}$	$k4_2f$	1.28 E-3	$\mu M^{-1} s^{-1}$	Estimate from K_m^*
FabG	$k_{off\text{-}\beta kaACP}$	$k4_2r$	2.17 E-2	s^{-1}	Used $k_{off\text{-}ACP}$ from FabD
FabG	k_{cat}	$kcat4$	5.90 E-1	s^{-1}	¹⁸

*Here, we used Eqs. 1 and 2 from the main text.

For these estimates, we used a measured value of k_{off} for the complex between C_4 acyl-CoA and FabI.*To clarify, we used k_{cat} as an order-of-magnitude estimate of the forward acyl-transfer constant.****For this estimate, we assumed a rate constant approximately tenfold higher than $k_{on\text{-}mCoA}$.

Table S4 (cont.). Estimates of Kinetic Parameters.

Enzyme	Parameter	Model Label	Value	Units	Source
FabZ	$K_{M-\beta\text{haACP}}$	N/A	5.60 E1	μM	²⁰
FabZ	$k_{\text{on}-\beta\text{haACP}}$	k_5_1f	3.88 E-4	$\mu\text{M}^{-1} \text{s}^{-1}$	Estimate from K_m^*
FabZ	$k_{\text{off}-\beta\text{haACP}}$	k_5_1r	2.17 E-2	s^{-1}	Used $k_{\text{off}-\text{ACP}}$ from FabD
FabZ	k_{cat}	$k_{\text{cat}5}$	2.72 E-1	s^{-1}	⁹
FabI	$K_{M_I_NADH}$	N/A	2.0 E-2	mM	²¹
FabI	$k_{\text{on}-I_NADH}$	k_6_1f	1.54 E-3	$\mu\text{M}^{-1} \text{s}^{-1}$	¹³
FabI	$k_{\text{off}-I_NADH}$	k_6_1r	7.93 E-2	s^{-1}	¹³
FabI	$K_{M-eacACP}$	N/A	2.0 E-2	mM	²²
FabI	$k_{\text{on}-eacACP}$	k_6_2f	1.09 E-3	$\mu\text{M}^{-1} \text{s}^{-1}$	Estimate from K_m^*
FabI	$k_{\text{off}-eacACP}$	k_6_2r	2.17 E-2	s^{-1}	Used $k_{\text{off}-\text{ACP}}$ from FabD
FabI	k_{cat}	$k_{\text{cat}6}$	4.0 E0	s^{-1}	²³
TesA	$k_{\text{on}-C4acACP}$	k_7_1f-C4	4.59 E-3	$\mu\text{M}^{-1} \text{s}^{-1}$	7, this study
TesA	$k_{\text{on}-C6acACP}$	k_7_1f-C6	7.38 E-3	$\mu\text{M}^{-1} \text{s}^{-1}$	7, this study
TesA	$k_{\text{on}-C8acACP}$	k_7_1f-C8	4.10 E-2	$\mu\text{M}^{-1} \text{s}^{-1}$	7, this study
TesA	$k_{\text{on}-C10acACP}$	k_7_1f-C10	1.47 E-1	$\mu\text{M}^{-1} \text{s}^{-1}$	7, this study
TesA	$k_{\text{on}-C12acACP}$	k_7_1f-C12	3.03 E-1	$\mu\text{M}^{-1} \text{s}^{-1}$	7, this study
TesA	$k_{\text{on}-C14acACP}$	k_7_1f-C14	5.42 E-1	$\mu\text{M}^{-1} \text{s}^{-1}$	7, this study
TesA	$k_{\text{on}-C16acACP}$	k_7_1f-C16	0.96669	$\mu\text{M}^{-1} \text{s}^{-1}$	7, this study
TesA	$k_{\text{on}-C18acACP}$	k_7_1f-C18	1.73 E0	$\mu\text{M}^{-1} \text{s}^{-1}$	7, this study
TesA	$k_{\text{on}-C20acACP}$	k_7_1f-C20	3.08 E0	$\mu\text{M}^{-1} \text{s}^{-1}$	7, this study
TesA	$k_{\text{off}-acACP}$	k_7_1r	2.17E0	s^{-1}	**
TesA	$k_{\text{cat}-C4}$	$k_{\text{cat}7-C4}$	6.13 E0	s^{-1}	7, this study
TesA	$k_{\text{cat}-C6}$	$k_{\text{cat}7-C6}$	5.50 E0	s^{-1}	7, this study
TesA	$k_{\text{cat}-C8}$	$k_{\text{cat}7-C8}$	1.12 E1	s^{-1}	7, this study
TesA	$k_{\text{cat}-C10}$	$k_{\text{cat}7-C10}$	1.71 E0	s^{-1}	7, this study
TesA	$k_{\text{cat}-C12}$	$k_{\text{cat}7-C12}$	2.73 E1	s^{-1}	7, this study
TesA	$k_{\text{cat}-C14}$	$k_{\text{cat}7-C14}$	4.95 E1	s^{-1}	7, this study
TesA	$k_{\text{cat}-C16}$	$k_{\text{cat}7-C16}$	1.08 E2	s^{-1}	7, this study
TesA	$k_{\text{cat}-C18}$	$k_{\text{cat}7-C18}$	1.32 E2	s^{-1}	7, this study
TesA	$k_{\text{cat}-C20}$	$k_{\text{cat}7-C20}$	1.66 E2	s^{-1}	7, this study
FabF	K_{M-F_acACP}	N/A	1.40 E-2	mM	²⁴
FabF	$k_{\text{on}-F_acACP}$	k_8_1f	1.55 E-3	$\mu\text{M}^{-1} \text{s}^{-1}$	Estimate from K_m^*
FabF	$k_{\text{off}-F_acACP}$	k_8_1r	2.17 E-2	s^{-1}	Used $k_{\text{off}-\text{ACP}}$ from FabD
FabF	$k_{\text{fwdFabF}*}$	k_8_2f	1.58 E3	s^{-1}	Used k_{f-FabD} from FabD***
FabF	$k_{\text{rvsFabF}*}$	k_8_2r	1.0 E-2	$\mu\text{M}^{-1} \text{s}^{-1}$	****
FabF	K_{M-F_mACP}		8.20 E-3	mM	²⁵
FabF	$k_{\text{on}-F_mACP}$	k_8_3f	2.65 E-3	$\mu\text{M}^{-1} \text{s}^{-1}$	Estimate from K_m^*
FabF	$k_{\text{off}-F_mACP}$	k_8_3r	2.17 E-2	s^{-1}	Used k_{f-FabD} from FabD***
FabF	k_{cat}	$k_{\text{cat}8}$	2.90 E-2	s^{-1}	²⁵

*Here, we used Eqs. 1 and 2 from the main text.

For these estimates, we used a measured value of k_{off} for the complex between C₄ acyl-CoA and FabI.*To clarify, we used k_{cat} as an order-of-magnitude estimate of the forward acyl-transfer constant.****For this estimate, we assumed a rate constant approximately tenfold higher than $k_{\text{on}-m\text{CoA}}$.

Table S5. Ranges of Kinetic Parameters.

Enzyme	Parameter	Value	Units	Source (low)	Source (high)
FabD	K_{M-mCoA}	6.0E1 – 2.50E2	μM	¹²	¹⁴
FabD	$k_{on-mCoA}$	1.28E-3 – 1.85E1	$\mu M^{-1} s^{-1}$	¹³	26, this study*
FabD	$k_{off-mCoA}$	8.0E-2 – 1.11E3	s^{-1}	¹³	Calculated from maximum K_m and k_{on}
FabD	k_{f-FabD^*}	9.34E-4 – 5.20E3	s^{-1}	^{14,26,27}	12,26, this study*
FabD	k_{r-FabD^*}	1.28E-3 – 1.85E1	$\mu M^{-1} s^{-1}$	¹³	26, this study*
FabD	K_{M-ACP}	4.0E1 – 3.51E2	μM	¹²	¹⁴
FabD	k_{on-ACP}	5.02E-2 – 3.70E0	$\mu M^{-1} s^{-1}$	¹⁵	1, this study*
FabD	$k_{off-ACP}$	2.17E-2 – 1.30E3	s^{-1}	¹⁵	Calculated from maximum K_m and k_{on}
FabD	k_{fFabD^*ACP}	9.34E-4 – 5.20E3	s^{-1}	^{14,26,27}	12,26, this study*
FabD	k_{rFabD^*ACP}	1.28E-3 – 3.70E0	$\mu M^{-1} s^{-1}$	¹³	1, this study*
FabD	k_{cat}	4.67E-4 – 2.60E3	s^{-1}	^{14,27}	¹²
FabH	K_{M-aCoA}	4.0E1 – 6.0E1	μM	¹⁶	¹²
FabH	$k_{on-aCoA}$	1.28E-3 – 1.87E1	$\mu M^{-1} s^{-1}$	¹³	26, this study*
FabH	$k_{off-aCoA}$	8.0E-2 – 1.12E3	s^{-1}	¹³	Calculated from maximum K_m and k_{on}
FabH	k_{f-FabH^*}	9.34E-4 – 5.20E3	s^{-1}	^{14,26,27}	12,26, this study*
FabH	k_{r-FabH^*}	1.28E-3 – 3.70E0	$\mu M^{-1} s^{-1}$	¹³	1, this study*
FabH	K_{M-mACP}	5.0E0 – 2.0E1	μM	¹⁶	¹²
FabH	$k_{on-mACP}$	5.02E-2 – 3.70E0	$\mu M^{-1} s^{-1}$	¹⁵	1, this study*
FabH	$k_{off-mACP}$	2.17E-2 – 7.40E1	s^{-1}	¹⁵	Calculated from maximum K_m and k_{on}
FabH	k_{cat}	2.7E-1 – 4.71E1	s^{-1}	¹⁶	^{12,17}
FabG	$K_{M-NADPH}$	1.0E1	μM	¹⁸	N/A
FabG	$k_{on-NADPH}$	1.54E-3 – 2.16E1	$\mu M^{-1} s^{-1}$	¹³	26, this study*
FabG	$k_{off-NADPH}$	7.90E-2 – 2.16E2	s^{-1}	¹³	Calculated from maximum K_m and k_{on}
FabG	$K_{M-\beta kaACP}$	3.60E0 – 7.50E1	μM	¹⁹	¹⁸
FabG	$k_{on-\beta kaACP}$	5.02E-2 – 3.70E0	$\mu M^{-1} s^{-1}$	¹⁵	1, this study*
FabG	$k_{off-\beta kaACP}$	2.17E-2 – 2.78E2	s^{-1}	¹⁵	Calculated from maximum K_m and k_{on}
FabG	k_{cat}	1.40E-2 – 2.65E2	s^{-1}	¹⁸	²⁸
FabZ	$k_{on-\beta haACP}$	5.02E-2 – 3.70E0	$\mu M^{-1} s^{-1}$	¹⁵	1, this study*
FabZ	$k_{off-\beta haACP}$	2.17E-2 – 2.07E2	s^{-1}	¹⁵	Calculated from maximum K_m and k_{on}
FabZ	k_{cat}	7.80E-2 – 7.20E1	s^{-1}	²⁰	^{9,29}

*We used the diffusion calculations described in SI Note 1.

Table S5 (cont.). Ranges of Kinetic Parameters.

Enzyme	Parameter	Value	Units	Source (low)	Source (high)
FabI	K_{M-I_NADPH}	2.0E1 – 5.16E1	μM	21	13
FabI	k_{on-I_NADPH}	1.54E-3 – 2.16E1	$\mu M^{-1} s^{-1}$	13	26, this study*
FabI	k_{off-I_NADPH}	7.93E-2 – 2.16E-1	s^{-1}	13	Calculated from maximum K_m and k_{on}
FabI	$K_{M-eacACP}$	3.0E1 – 6.25E1	μM	21	13
FabI	$k_{on-eacACP}$	5.02E-2 – 3.70E0	$\mu M^{-1} s^{-1}$	15	1, this study*
FabI	$k_{off-eacACP}$	2.17E-2 – 2.31E2	s^{-1}	15	Calculated from maximum K_m and k_{on}
FabI	k_{cat}	2.50E-1 – 1.30E2	s^{-1}	21,30	31
TesA	$K_{M-C16acACP}$	4.0E0 – 1.09E3	μM	32	7
TesA	$k_{on-acACP}$	5.02E-2 – 3.70E0	$\mu M^{-1} s^{-1}$	15	1, this study*
TesA	$k_{off-acACP}$	2.17E-2 – 4.04E3	s^{-1}	15	Calculated from maximum K_m and k_{on}
TesA	$k_{cat-C16}$	8.0E-3 – 1.08E2	s^{-1}	33	7
FabF	K_{M-F_acACP}	8.20E0 – 4.0E1	μM	25	24
FabF	k_{on-F_acACP}	5.02E-2 – 3.70E0	$\mu M^{-1} s^{-1}$	15	1, this study*
FabF	k_{off-F_acACP}	2.17E-2 – 1.48E2	s^{-1}	15	Calculated from maximum K_m and k_{on}
FabF	$k_{fwdFabF^*}$	9.34E-4 – 5.20E3	s^{-1}	14,26,27	12,26, this study*
FabF	$k_{rvsFabF^*}$	1.28E-3 – 3.70E0	$\mu M^{-1} s^{-1}$	13	1, this study*
FabF	K_{M-F_mACP}	8.2E0 – 4.0E1	μM	25	24
FabF	k_{on-F_mACP}	5.02E-2 – 3.70E0	$\mu M^{-1} s^{-1}$	15	1, this study*
FabF	k_{off-F_mACP}	2.17E-2 – 1.48E2	s^{-1}	15	Calculated from maximum K_m and k_{on}
FabF	k_{cat}	2.9E-2 – 5.51E2	s^{-1}	25	34

*We used the diffusion calculations described in SI Note 1.

Table S6. Optimized Scaling Parameters for the Kinetic Model.

Parameter	Description*	Estimated Range**	Optimized Value***
a₁	Scales k _{off} for 1-4	1E0 to 1.4E4	4.498 E3
a₂	Scales k _{off} for acyl-ACPs for 5-11	1E0 to 1.28E4	1.586 E1
a₃	Scales k _{off} for 12	1E0 to 1.86E5	4.319 E3
b₁	Scales k _r for 1-3 and 10	0.128 to 3.7E2	2.474 E1
b₂	Scales K _{eq} for acyl transfer in 1	2.46E-7 to 1.98E3	5.277 E-2
b₃	Scales K _{eq} for acyl transfer in 2, 3, 10	2.46E-7 to 3.96E2	8.541 E-2
c₁	Scales k _{cat} for 4	1E-3 to 1.5E1	1.651 E0
c₂	Scales k _{cat} for 6, 7, 9, 11	1E-2 to 2.4E2	8.794 E1
c₃	Scales k _{cat} for 12	7.45E-5 to 1E0	1.902 E-2
d₁	Substrate specificity of TesA; see Eq. 3 in main text.	-5E-1 to 5E-1	-2.897 E-1
d₂	Substrate specificity of TesA; see Eq. 3 of main text.	0 to 1E1	5.443 E0
e	Scales inhibition of (i) FabH/ F by holo-ACPS and (ii) FabH by acyl-ACPs.	1E0 to 9E2	2.872 E1

*The numbers in these descriptions correspond to reactions in Table 1.

**We determined these ranges from the ranges of associated scaled parameters described in Table S5.

***We determined these parameters by optimizing our kinetic model.

Table S7. Optimized Binding Parameters for ACPs and Acyl-ACPs.

Enzyme	Substrate	K_D (μM)	k_{on} (μM⁻¹ s⁻¹)	k_{off} (s⁻¹)
FabH	ACP	3.14E1	6.92E-4	2.17E-2
FabH	C ₄ / C ₆ / C ₈ /C ₁₀ -ACP	1.51E2	3.09E-1	4.66E1
FabH	C ₁₂ -ACP	1.51E2	3.09E-1	4.66E1
FabH	C ₁₄ -ACP	2.87E1	3.09E-1	8.87E0
FabH	C ₁₆ -ACP	3.37E1	3.09E-1	1.04E1
FabH	C ₁₈ -ACP	8.76E0	3.09E-1	2.70E0
FabH	C ₂₀ -ACP	4.48E0	3.09E-1	1.38E0
FabH*	C ₄ / C ₆ / C ₈ /C ₁₀ -ACP	8.24E-1	1.55E0	1.28E0
FabH*	C ₁₂ -ACP	8.24E-1	1.55E0	1.28E0
FabH*	C ₁₄ -ACP	1.05E0	1.55E0	1.63E0
FabH*	C ₁₆ -ACP	2.63E-1	1.55E0	4.08E-1
FabH*	C ₁₈ -ACP	2.95E-1	1.55E0	4.58E-1
FabH*	C ₂₀ -ACP	8.74E-2	1.55E0	1.36E-1
TesA	holo-ACP	9.00E0	2.41E-3	2.17E-2
FabG	holo-ACP	9.00E0	2.41E-3	2.17E-2
FabZ	holo-ACP	9.00E0	2.41E-3	2.17E-2
FabI	holo-ACP	9.00E0	2.41E-3	2.17E-2
FabF	holo-ACP	3.14E-1	6.92E-2	2.17E-2

*ACP refers to holo-ACP; C_i-ACP refers to an acyl-ACP with *i* carbons in its acyl chain.

*We determined these parameters by optimizing our kinetic model.

Table S8. Optimized Kinetic Parameters for Various Thioesterases

Enzyme	Substrate	k _{cat} (1/s)	K _D (μ M)
BfTES	C ₄ -ACP	2.35	1.45
BfTES	C ₆ -ACP	1.70	2.62
BfTES	C ₈ -ACP	1.05	4.73
BfTES	C ₁₀ -ACP	0.40	8.53
CpFatB1	C ₆ -ACP	0.105	274
CpFatB1	C ₈ -ACP	2.77	0.989
CpFatB1	C ₁₀ -ACP	0.033	13.8
UcFatB	C ₁₀ -ACP	0.105	274
UcFatB	C ₁₂ -ACP	1.37	3.52
UcFatB	C ₁₄ -ACP	0.033	13.8

*C_i-ACP refers to an acyl-ACP with *i* carbons in its acyl chain.

**We determined these parameters by optimizing our kinetic model.

Table S9. Sensitivity Analysis of Scaling Parameters.

Objective	Parameter	Min	Max	EE Mean	EE SD	Mean/SD
Avg. Length	d ₂	0	10	11.34	3.40	0.30
Avg. Length	d ₁	-0.5	0	7.08	2.64	0.37
Avg. Length	c ₂	1	240	4.16	10.42	2.50
Avg. Length	c ₃	1.00E-03	0.1	3.71	4.18	1.13
Avg. Length	e	0.1	200	2.61	2.86	1.10
Avg. Length	b ₁	1	100	1.89	2.57	1.36
Avg. Length	b ₃	1.00E-03	0.1	1.18	1.13	0.96
Avg. Length	c ₁	0.1	15	0.97	1.82	1.87
Avg. Length	b ₂	1.00E-03	0.1	0.89	0.91	1.02
Avg. Length	a ₁	100	10000	0.65	0.60	0.92
Avg. Length	a ₂	1	100	0.30	0.36	1.21
Avg. Length	a ₃	100	10000	0.11	0.32	2.91
Production	c ₂	1	240	32.56	72.69	2.23
Production	b ₁	1	100	32.23	49.22	1.53
Production	b ₃	1.00E-03	0.1	22.28	25.47	1.14
Production	d ₂	0	10	20.00	22.60	1.13
Production	b ₂	1.00E-03	0.1	17.94	19.36	1.08
Production	d ₁	-0.5	0	17.03	28.11	1.65
Production	a ₁	100	10000	16.08	17.82	1.11
Production	c ₁	0.1	15	12.81	46.01	3.59
Production	c ₃	1.00E-03	0.1	9.19	15.85	1.72
Production	e	0.1	200	4.98	6.70	1.35
Production	a ₃	100	10000	1.10	7.89	7.16
Production	a ₂	1	100	0.39	0.49	1.26
Obj _A	d ₂	0	10	4.29E05	5.39E05	1.26
Obj _A	d ₁	-0.5	0	3.28E05	4.40E05	1.34
Obj _A	b ₃	1.00E-03	0.1	1.97E05	3.59E05	1.82
Obj _A	b ₁	1	100	1.69E05	3.32E05	1.96
Obj _A	c ₃	1.00E-03	0.1	1.69E05	2.28E05	1.35
Obj _A	c ₂	1	240	1.64E05	3.29E05	2.01
Obj _A	b ₂	1.00E-03	0.1	1.59E05	2.70E05	1.70
Obj _A	e	0.1	200	1.39E05	2.15E05	1.55
Obj _A	a ₁	100	10000	1.15E05	1.57E05	1.37
Obj _A	c ₁	0.1	15	8.90E04	2.07E05	2.33
Obj _A	a ₃	100	10000	1.62E04	1.03E05	6.34
Obj _A	a ₂	1	100	5.55E03	6.92E03	1.25

*This table shows the mean elementary effects used to generate Figure 9A.

**Obj_A is described in Materials and Methods.

Appendix 1. Model Equations*

$$[\text{FabD}] = [\text{FabD}]_{\text{tot}} - [\text{FabD} \cdot \text{Malonyl-CoA}] - [\text{FabD}^*] - [\text{FabD}^* \cdot \text{ACP}] \quad \text{Eq. S4}$$

$$[\text{FabH}] = [\text{FabH}]_{\text{tot}} - [\text{FabH} \cdot \text{Acetyl-CoA}] - [\text{FabH}^*] - [\text{FabH}^* \cdot \text{Malonyl-ACP}] \quad \text{Eq. S5}$$

$$[\text{FabH}] = [\text{FabH}]_{\text{tot}} - [\text{FabH} \cdot \text{Acetyl-CoA}] - [\text{FabH}^*] - [\text{FabH}^* \cdot \text{Malonyl-ACP}] \\ - \sum_{n=2}^{10} [\text{FabH} \cdot C_{2n}\text{Acyl-ACP}] - \sum_{n=2}^{10} [\text{FabH}^* \cdot C_{2n}\text{Acyl-ACP}] - [\text{FabH} \cdot \text{ACP}]$$

$$[\text{FabG}] = [\text{FabG}]_{\text{tot}} - [\text{FabG} \cdot \text{NADPH}] - \sum_{n=2}^{10} [\text{FabG} \cdot \text{NADPH} \cdot C_{2n}\beta\text{-ketoacyl-ACP}] \\ - [\text{FabG} \cdot \text{ACP}] \quad \text{Eq. S6}$$

$$[\text{FabZ}] = [\text{FabZ}]_{\text{tot}} - \sum_{n=2}^{10} [\text{FabZ} \cdot C_{2n}\beta\text{-hydroxyacyl-ACP}] - [\text{FabZ} \cdot \text{ACP}] \quad \text{Eq. S7}$$

$$[\text{FabI}] = [\text{FabI}]_{\text{tot}} - [\text{FabI} \cdot \text{NADH}] - \sum_{n=2}^{10} [\text{FabI} \cdot \text{NADH} \cdot C_{2n}\text{Enoylacyl-ACP}] - [\text{FabI} \cdot \text{ACP}] \quad \text{Eq. S8}$$

$$[\text{TesA}] = [\text{TesA}]_{\text{tot}} - \sum_{n=2}^{10} [\text{TesA} \cdot C_{2n}\text{acyl-ACP}] - [\text{TesA} \cdot \text{ACP}] \quad \text{Eq. S9}$$

$$[\text{FabF}] = [\text{FabF}]_{\text{tot}} - \sum_{n=2}^{10} [\text{FabF} \cdot C_{2n}\text{acyl-ACP}] - \sum_{n=2}^{10} [C_{2n}\text{FabF}^*] \\ - \sum_{n=2}^{10} [C_{2n}\text{FabF}^* \cdot \text{Malonyl-ACP}] - [\text{FabF} \cdot \text{ACP}] \quad \text{Eq. S10}$$

$$\frac{d[\text{Acetyl-CoA}]}{dt} = k_{\text{off-aCoA}}[\text{FabH} \cdot \text{Acetyl-CoA}] - k_{\text{on-aCoA}}[\text{FabH}][\text{Acetyl-CoA}] \quad \text{Eq. S11}$$

$$\frac{d[\text{ACP}]}{dt} = k_{\text{off-ACP}}[\text{FabD}^* \cdot \text{ACP}] - k_{\text{on-ACP}}[\text{FabD}^*][\text{ACP}] \\ + \sum_{n=2}^{10} k_{\text{catTesA,C2n}}[\text{TesA} \cdot C_{2n}\text{Acyl-ACP}] + \sum_{n=2}^{10} k_{\text{f-FabF}^*}[\text{FabF}][C_{2n}\text{Acyl-ACP}] \\ - \sum_{n=2}^{10} k_{\text{r-FabF}^*}[C_{2n}\text{FabF}^*][\text{ACP}] + k_{\text{off-FabH-Inh-l}}[\text{FabH} \cdot \text{ACP}] \\ - k_{\text{on-FabH-Inh-l}}[\text{FabH}][\text{ACP}] + k_{\text{off-FabG-Inh}}[\text{FabG} \cdot \text{ACP}] \\ - k_{\text{on-FabG-Inh}}[\text{FabG}][\text{ACP}] + k_{\text{off-FabZ-Inh}}[\text{FabZ} \cdot \text{ACP}] - k_{\text{on-FabZ-Inh}}[\text{FabZ}][\text{ACP}] \\ + k_{\text{off-FabI-Inh}}[\text{FabI} \cdot \text{ACP}] - k_{\text{on-FabI-Inh}}[\text{FabI}][\text{ACP}] + k_{\text{off-TesA-Inh}}[\text{TesA} \cdot \text{ACP}] \\ - k_{\text{on-TesA-Inh}}[\text{TesA}][\text{ACP}] + k_{\text{off-FabF-Inh}}[\text{FabF} \cdot \text{ACP}] - k_{\text{on-FabF-Inh}}[\text{FabF}][\text{ACP}] \quad \text{Eq. S12}$$

$$\frac{d[\text{NADPH}]}{dt} = k_{\text{off-NADPH}}[\text{FabG} \cdot \text{NADPH}] - k_{\text{on-NADPH}}[\text{FabG}][\text{NADPH}] \quad \text{Eq. S13}$$

*Legend: In these equations, ACP refers to holo-ACP. For Eq. S20, n = 3-10; for Eq. S21-S23, S31-S32, S34, and S38-S39, n = 2-10; and for Eq. S35-37, n = 2-9.

$$\frac{d[NADH]}{dt} = k_{off-NADH}[FabI \cdot NADH] - k_{on-NADH}[FabI][NADH] \quad Eq. S14$$

$$\frac{d[Malonyl-CoA]}{dt} = k_{off-mCoA}[FabD \cdot Malonyl-CoA] - k_{on-mCoA}[FabD][Malonyl-CoA] \quad Eq. S15$$

$$\begin{aligned} \frac{d[CoA]}{dt} = & k_{f-FabD^*}[FabD \cdot Malonyl-CoA] - k_{r-FabD^*}[FabD^*][CoA] \\ & - k_{f-FabH^*}[FabH][Acetyl-CoA] - k_{r-FabH^*}[FabD][Acetyl-CoA] \end{aligned} \quad Eq. S16$$

$$\begin{aligned} \frac{d[Malonyl-ACP]}{dt} = & k_{f-FabD^*ACP}[FabD^* \cdot ACP] - k_{r-FabD^*ACP}[FabD][ACP] \\ & - k_{on-mACP}[FabH^*][Malonyl-ACP] - k_{off-mACP}[FabH^* \cdot Malonyl-ACP] \\ & + \sum_{n=2}^9 k_{off-FmACP}[C_{2n}FabF^* \cdot Malonyl-ACP] \\ & - \sum_{n=2}^9 k_{on-F_mACP}[C_{2n}FabF^*][Malonyl-ACP] \end{aligned} \quad Eq. S17$$

$$\frac{d[CO_2]}{dt} = k_{catFabH}[FabH^* \cdot Malonyl-ACP] + \sum_{n=2}^{10} k_{catFabF}[C_{2n}FabF^* \cdot Malonyl-ACP] \quad Eq. S18$$

$$\begin{aligned} \frac{d[C_4\beta-ketoacyl-ACP]}{dt} = & k_{catFabH}[FabH^* \cdot Malonyl-ACP] \\ & + k_{off\beta kaACP}[FabG \cdot NADPH \cdot C_4\beta-ketoacyl-ACP] \\ & - k_{on\beta kaACP}[FabG \cdot NADPH][C_4\beta-ketoacyl-ACP] \end{aligned} \quad Eq. S19$$

$$\begin{aligned} \frac{d[C_{2n}\beta-ketoacyl-ACP]}{dt} = & k_{off\beta kaACP}[FabG \cdot NADPH \cdot C_{2n}\beta-ketoacyl-ACP] \\ & - k_{on\beta kaACP}[FabG \cdot NADPH][C_{2n}\beta-ketoacyl-ACP] \\ & + k_{catFabF}[C_{2n}FabF^* \cdot Malonyl-ACP] \end{aligned} \quad Eq. S20$$

$$\begin{aligned} \frac{d[C_{2n}\beta-hydroxyacyl-ACP]}{dt} = & k_{off\beta haACP}[FabZ \cdot C_{2n}\beta-hydroxyacyl-ACP] \\ & - k_{on\beta haACP}[FabZ][C_{2n}\beta-hydroxyacyl-ACP] \\ & + k_{catFabG}[FabG \cdot NADPH \cdot C_{2n}\beta-ketoacyl-ACP] \end{aligned} \quad Eq. S21$$

$$\begin{aligned} \frac{d[C_{2n}Enoylacyl-ACP]}{dt} = & k_{off-eacACP}[FabI \cdot NADH \cdot C_{2n}Enoylacyl-ACP] \\ & - k_{on-eacACP}[FabI \cdot NADH][C_{2n}Enoylacyl-ACP] \\ & + k_{catFabZ}[FabZ \cdot C_{2n}\beta-hydroxyacyl-ACP] \end{aligned} \quad Eq. S22$$

$$\frac{d[C_{2n}\text{acyl-ACP}]}{dt} = k_{\text{catFabI}}[\text{FabI} \cdot \text{NADH} \cdot C_{2n}\text{Enoylacyl-ACP}] + k_{\text{catFabI}}[\text{FabI} \cdot \text{NADH} \cdot C_{2n}\text{Enoylacyl-ACP}] - k_{\text{on-FacACP}}[\text{FabF}][C_{2n}\text{Acyl-ACP}] + k_{\text{off-FabH-Inh-2}}[\text{FabH} \cdot C_{2n}\text{Acyl-ACP}] - k_{\text{on-FabH-Inh-2,C2n}}[\text{FabH}][C_{2n}\text{Acyl-ACP}] + k_{\text{off-FabH-Inh-3}}[\text{FabH}^* \cdot C_{2n}\text{Acyl-ACP}] - k_{\text{on-FabH-Inh-3,C2n}}[\text{FabH}^*][C_{2n}\text{Acyl-ACP}] \quad \text{Eq. S23}$$

$$\frac{d[\text{FabD} \cdot \text{Malonyl-CoA}]}{dt} = k_{\text{on-mCoA}}[\text{FabD}][\text{Malonyl-CoA}] - k_{\text{off-mCoA}}[\text{FabD} \cdot \text{Malonyl-CoA}] + k_{\text{r-FabD}^*}[\text{FabD}^*][\text{CoA}] - k_{\text{f-FabD}^*}[\text{FabD} \cdot \text{Malonyl-CoA}] \quad \text{Eq. S24}$$

$$\frac{d[\text{FabD}^*]}{dt} = k_{\text{f-FabD}^*}[\text{FabD} \cdot \text{Malonyl-CoA}] - k_{\text{r-FabD}^*}[\text{FabD}^*][\text{CoA}] + k_{\text{off-ACP}}[\text{FabD}^* \cdot \text{ACP}] - k_{\text{on-ACP}}[\text{FabD}^*][\text{ACP}] \quad \text{Eq. S25}$$

$$\frac{d[\text{FabD}^* \cdot \text{ACP}]}{dt} = k_{\text{on-ACP}}[\text{FabD}^*][\text{ACP}] - k_{\text{off-ACP}}[\text{FabD}^* \cdot \text{ACP}] + k_{\text{r-FabD}^*\text{ACP}}[\text{FabD}][\text{Malonyl-ACP}] - k_{\text{f-FabD}^*\text{ACP}}[\text{FabD}^* \cdot \text{ACP}] \quad \text{Eq. S26}$$

$$\frac{d[\text{FabH} \cdot \text{Acetyl-CoA}]}{dt} = k_{\text{on-aCoA}}[\text{FabH}][\text{Acetyl-CoA}] - k_{\text{off-aCoA}}[\text{FabH} \cdot \text{Acetyl-CoA}] + k_{\text{r-FabH}^*}[\text{FabH}^*][\text{CoA}] - k_{\text{f-FabH}^*}[\text{FabH} \cdot \text{Acetyl-CoA}] \quad \text{Eq. S27}$$

$$\frac{d[\text{FabH}^*]}{dt} = k_{\text{f-FabH}^*}[\text{FabH} \cdot \text{Acetyl-CoA}] - k_{\text{r-FabH}^*}[\text{FabH}^*][\text{CoA}] + k_{\text{off-mACP}}^{10}[\text{FabH}^* \cdot \text{Malonyl-ACP}] - k_{\text{on-mACP}}[\text{FabH}^*][\text{Malonyl-ACP}] + \sum_{n=2}^{10} k_{\text{off-FabH-Inh-3,C2n}}[\text{FabH}^* \cdot C_{2n}\text{Acyl-ACP}] - \sum_{n=2}^{10} k_{\text{on-FabH-Inh-3,C2n}}[\text{FabH}^*][C_{2n}\text{Acyl-ACP}] \quad \text{Eq. S28}$$

$$\frac{d[\text{FabH}^* \cdot \text{Malonyl-ACP}]}{dt} = k_{\text{on-mACP}}[\text{FabH}^*][\text{Malonyl-ACP}] - k_{\text{off-mACP}}[\text{FabH}^* \cdot \text{Malonyl-ACP}] - k_{\text{catFabH}}[\text{FabH}^* \cdot \text{Malonyl-ACP}] \quad \text{Eq. S29}$$

$$\frac{d[\text{FabG} \cdot \text{NADPH}]}{dt} = k_{\text{on-NADPH}}^{10}[\text{FabG}][\text{NADPH}] - k_{\text{off-NADPH}}[\text{FabG} \cdot \text{NADPH}] + \sum_{n=2}^{10} k_{\text{off}\beta\text{kaACP}}[\text{FabG} \cdot \text{NADPH} \cdot C_{2n}\beta\text{-ketoacyl-ACP}] - \sum_{n=2}^{10} k_{\text{on}\beta\text{kaACP}}[\text{FabG} \cdot \text{NADPH}][C_{2n}\beta\text{-ketoacyl-ACP}] \quad \text{Eq. S30}$$

$$\frac{d[FabG \cdot NADPH \cdot C_{2n}\beta\text{-ketoacyl-ACP}]}{dt} = k_{on\beta kaACP}[FabG \cdot NADPH][C_{2n}\beta\text{-ketoacyl-ACP}] - k_{off\beta kaACP}[FabG \cdot NADPH \cdot C_{2n}\beta\text{-ketoacyl-ACP}] - k_{catFabG}[FabG \cdot NADPH \cdot C_{2n}\beta\text{-ketoacyl-ACP}]$$

Eq. S31

$$\frac{d[FabZ \cdot C_{2n}\beta\text{-hydroxyacyl-ACP}]}{dt} = k_{on\beta haACP}[FabZ][C_{2n}\beta\text{-hydroxyacyl-ACP}] - k_{off\beta haACP}[FabZ \cdot C_{2n}\beta\text{-hydroxyacyl-ACP}] - k_{catFabZ}[FabZ \cdot C_{2n}\beta\text{-hydroxyacyl-ACP}]$$

Eq. S32

$$\frac{d[FabI \cdot NADH]}{dt} = k_{on-NADH}[FabI][NADH] - k_{off-NADPH}[FabI \cdot NADH] + \sum_{n=2}^{10} k_{off-eacACP}[FabI \cdot NADH \cdot C_{2n}\text{Enoylacyl-ACP}] - \sum_{n=2}^{10} k_{on-eacACP}[FabI \cdot NADH][C_{2n}\text{Enoylacyl-ACP}]$$

Eq. S33

$$\frac{d[TesA \cdot C_{2n}\text{acyl-ACP}]}{dt} = k_{on-acACP}[TesA][C_{2n}\text{Acyl-ACP}] - k_{off-acACP}[TesA \cdot C_{2n}\text{Acyl-ACP}] - k_{catTesA}[TesA \cdot C_{2n}\text{Acyl-ACP}]$$

Eq. S34

$$\frac{d[FabF \cdot C_{2n}\text{acyl-ACP}]}{dt} = k_{on-F_acACP}[FabF][C_{2n}\text{Acyl-ACP}] - k_{off-F_acACP}[FabF \cdot C_{2n}\text{Acyl-ACP}] + k_{r-FabF^*}[C_{2n}\text{FabF}^*][ACP] - k_{f-FabF^*}[FabF \cdot C_{2n}\text{acyl-ACP}]$$

Eq. S35

$$\frac{d[C_{2n}\text{FabF}^*]}{dt} = k_{f-FabF^*}[FabF \cdot C_{2n}\text{acyl-ACP}] - k_{r-FabF^*}[C_{2n}\text{FabF}^*][ACP] + k_{off-F_mACP}[C_{2n}\text{FabF}^* \cdot \text{Malonyl-ACP}] - k_{on-F_mACP}[C_{2n}\text{FabF}^*][\text{Malonyl-ACP}]$$

Eq. S36

$$\frac{d[C_{2n}\text{FabF}^* \cdot \text{Malonyl-ACP}]}{dt} = k_{on-F_mACP}[C_{2n}\text{FabF}^*][\text{Malonyl-ACP}] - k_{off-F_mACP}[C_{2n}\text{FabF}^* \cdot \text{Malonyl-ACP}] - k_{catFabF}[C_{2n}\text{FabF}^* \cdot \text{Malonyl-ACP}]$$

Eq. S37

$$\frac{d[FabH \cdot C_{2n}\text{Acyl-ACP}]}{dt} = k_{on-FabH-Inh-2}[FabH][C_{2n}\text{Acyl-ACP}] - k_{off-FabH-Inh-2,C_{2n}}[FabH \cdot C_{2n}\text{Acyl-ACP}]$$

Eq. S38

$$\frac{d[FabH^* \cdot C_{2n}\text{Acyl-ACP}]}{dt} = k_{on-FabH-Inh-3}[FabH^*][C_{2n}\text{Acyl-ACP}] - k_{off-FabH-Inh-3,C_{2n}}[FabH^* \cdot C_{2n}\text{Acyl-ACP}]$$

Eq. S39

$$\frac{d[TesA \cdot ACP]}{dt} = k_{on-TesA-Inh}[TesA][ACP] - k_{off-TesA-Inh}[TesA \cdot ACP]$$

Eq. S40

$$\frac{d[FabH \cdot ACP]}{dt} = k_{on-FabH-Inh} [FabH][ACP] - k_{off-FabH-Inh} [FabH \cdot ACP] \quad Eq. S41$$

$$\frac{d[FabG \cdot ACP]}{dt} = k_{on-FabG-Inh} [FabG][ACP] - k_{off-FabG-Inh} [FabG \cdot ACP] \quad Eq. S42$$

$$\frac{d[FabZ \cdot ACP]}{dt} = k_{on-FabZ-Inh} [FabZ][ACP] - k_{off-FabZ-Inh} [FabZ \cdot ACP] \quad Eq. S43$$

$$\frac{d[FabI \cdot ACP]}{dt} = k_{on-FabI-Inh} [FabI][ACP] - k_{off-FabI-Inh} [FabI \cdot ACP] \quad Eq. S44$$

$$\frac{d[FabF \cdot ACP]}{dt} = k_{on-FabF-Inh} [FabF][ACP] - k_{off-FabF-Inh} [FabF \cdot ACP] \quad Eq. S45$$

Appendix 2. MATLAB Code and Associated Files

1. Combined_Pathway_Solver. This program initiates and solves the kinetic model with the specified input parameters and options described in files 2-8.
2. Combined_Pathway_Model. This program contains material balances and differential equations used to model FAS activity.
3. LeastSquaresCalc. This program calculates sums of squared errors between predicted and experimental trends (Experimental_Dataset.csv).
4. param_func. This file parameterizes the model with specified input parameters.
5. kcat.csv. This file contains the estimates of k_{cat} used by param_func.
6. km_est.csv. This file contains the estimates of K_m used by param_func.
7. est_param.csv. This file contains estimates of all ratios of k_{on} to k_{off} used by param_func.
8. Experimental_Dataset.csv: contains the digitized values of previously reported experimental data.⁴

SI References

- (1) Schlosshauer, M.; Baker, D. Realistic Protein-Protein Association Rates from a Simple Diffusional Model Neglecting Long-Range Interactions, Free Energy Barriers, and Landscape Ruggedness. *Protein Sci.* **2004**, *13*, 1660–1669.
- (2) Erickson, H. P. Size and Shape of Protein Molecules at the Nanometer Level Determined by Sedimentation, Gel Filtration, and Electron Microscopy. *Biol. Proced. Online* **2009**, *11*, 32–51.
- (3) Harpaz, Y.; Gerstein, M.; Chothia, C. Volume Changes on Protein Folding. *Structure*. **1994**, *2*, 641–649.
- (4) Yu, X.; Liu, T.; Zhu, F.; Khosla, C. In Vitro Reconstitution and Steady-State Analysis of the Fatty Acid Synthase from Escherichia Coli. *Proc. Natl. Acad. Sci.* **2011**, *108*, 18643–18648.
- (5) Jeon, E.; Lee, S.; Won, J. I.; Han, S. O.; Kim, J.; Lee, J. Development of Escherichia Coli MG1655 Strains to Produce Long Chain Fatty Acids by Engineering Fatty Acid Synthesis (FAS) Metabolism. *Enzyme Microb. Technol.* **2011**, *49*, 44–51.
- (6) Leskovac, V. *Comprehensive Enzyme Kinetics*; Kluwer Academic Publishers: New York, 2004.
- (7) Grisewood, M. J.; Hernández-Lozada, N. J.; Thoden, J. B.; Gifford, N. P.; Mendez-Perez, D.; Schoenberger, H. A.; Allan, M. F.; Floy, M. E.; Lai, R. Y.; Holden, H. M.; Pfleger, B. F.; Maranas, C. D. Computational Redesign of Acyl-ACP Thioesterase with Improved Selectivity toward Medium-Chain-Length Fatty Acids. *ACS Catal.* **2017**, *7*, 3837–3849.
- (8) Heath, R. J.; Rock, C. O.; Chem, C. O. J. B. Inhibition of B-Ketoacyl-Acyl Carrier Protein Synthase III (FabH) by Acyl-Acyl Carrier Protein in Escherichia Coli. *J. Biol. Chem.* **1996**, *271*, 10996–11000.
- (9) Heath, R. J.; Rock, C. O. Roles of the FabA and FabZ β -Hydroxyacyl-Acyl Carrier Protein Dehydratases in Escherichia Coli Fatty Acid Biosynthesis. *J. Biol. Chem.* **1996**, *271*, 27795–27801.
- (10) Choi, Y. J.; Lee, S. Y. Microbial Production of Short-Chain Alkanes. *Nature* **2013**, *502*, 571–574.
- (11) Torella, J. P.; Ford, T. J.; Kim, S. N.; Chen, A. M.; Way, J. C.; Silver, P. A. Tailored Fatty Acid Synthesis via Dynamic Control of Fatty Acid Elongation. *Proc. Natl. Acad. Sci. U. S. A.* **2013**, *110*, 11290–11295.
- (12) Marcella, A. M.; Barb, A. W. A Rapid Fluorometric Assay for the S-Malonyltransacylase FabD and Other Sulphydryl Utilizing Enzymes. *J Biol Methods* **2016**, *3*, 1–7.
- (13) Kapoor, M.; Mukhi, P. L. S.; Surolia, N.; Suguna, K.; Surolia, A. Kinetic and Structural Analysis of the Increased Affinity of Enoyl-ACP (Acyl-Carrier Protein) Reductase for Triclosan in the Presence of NAD⁺. *Biochem. J.* **2004**, *381*, 725–733.
- (14) Szafranska, A. E.; Hitchman, T. S.; Cox, R. J.; Crosby, J.; Simpson, T. J. Kinetic and Mechanistic Analysis of the Malonyl CoA:ACP Transacylase from Streptomyces Coelicolor Indicates a Single Catalytically Competent Serine Nucleophile at the Active Site. *Biochemistry* **2002**, *41*, 1421–1427.
- (15) Zhang, L.; Liu, W.; Xiao, J.; Hu, T.; Chen, J.; Chen, K.; Jiang, H.; Shen, X. Malonyl-CoA: Acyl Carrier Protein Transacylase from Helicobacter Pylori: Crystal Structure and Its Interaction with Acyl Carrier Protein. *Protein Sci* **2007**, *16*, 1184–1192.

- (16) Heath, R. J.; Rock, C. O. Inhibition of Beta-Ketoacyl-Acyl Carrier Protein Synthase III (FabH) by Acyl-Acyl Carrier Protein in Escherichia Coli. *J. Biol. Chem.* **1996**, *271*, 10996–11000.
- (17) Qiu, X.; Choudhry, A. E.; Janson, C. a; Grooms, M.; Daines, R. a; Lonsdale, J. T.; Khandekar, S. S. Crystal Structure and Substrate Specificity of the B-Ketoacyl-Acyl Carrier Protein Synthase III (FabH) from Staphylococcus Aureus. *Protein Sci.* **2005**, *14*, 2087–2094.
- (18) Sun, Y. H.; Cheng, Q.; Tian, W. X.; Wu, X. D. A Substitutive Substrate for Measurements of Beta-Ketoacyl Reductases in Two Fatty Acid Synthase Systems. *J. Biochem. Biophys. Methods* **2008**, *70*, 850–856.
- (19) Shimakata, T.; Stumpf, P. K. Isolation and Function of Spinach Leaf β -Ketoacyl-[Acyl-Carrier-Protein] Synthases. *Proc. Natl. Acad. Sci. U. S. A.* **1982**, *79*, 5808–5812.
- (20) Swarnamukhi, P. L.; Sharma, S. K.; Bajaj, P.; Surolia, N.; Surolia, A.; Suguna, K. Crystal Structure of Dimeric FabZ of Plasmodium Falciparum Reveals Conformational Switching to Active Hexamers by Peptide Flips. *FEBS Lett.* **2006**, *580*, 2653–2660.
- (21) Sivaraman, S.; Zwahlen, J.; Bell, A. F.; Hedstrom, L.; Tonge, P. J. Structure-Activity Studies of the Inhibition of FabI, the Enoyl Reductase from Escherichia Coli, by Triclosan: Kinetic Analysis of Mutant FabIs. *Biochemistry* **2003**, *42*, 4406–4413.
- (22) Weeks, G.; Wakil, S. J. Mechanism of Fatty Acid Synthesis. XVIII. Preparation and General Properties of the Enoyl Acyl Carrier Protein Reductases from Escherichia Coli. *J. Biol. Chem.* **1968**, *243*, 1180–1189.
- (23) Liu, N.; Cummings, J. E.; England, K.; Slayden, R. A.; Tonge, P. J. Mechanism and Inhibition of the FabI Enoyl-ACP Reductase from Burkholderia Pseudomallei. *J. Antimicrob. Chemother.* **2011**, *66*, 564–573.
- (24) D’Agnolo, G.; Rosenfeld, I. S.; Vagelos, P. R. . Multiple Forms of Beta-Ketoacyl-Acyl Carrier Protein Synthetase in Escherichia Coli. *J. Biol. Chem.* **1975**, *250*, 5289–5294.
- (25) Borgaro, J.; Chang, a; Machutta, C.; Zhang, X.; Tonge, P. J. Substrate Recognition by Beta-Ketoacyl-ACP Synthases. *Biochemistry* **2011**, *50*, 10678–10686.
- (26) Mavrovouniotis, M. L.; Stephanopoulos, G. Estimation of Upper Bounds for the Rates of Enzymatic Reactions. *Chem. Eng. Commun.* **1990**, *93*, 211–236.
- (27) Misra, A.; Surolia, N.; Surolia, A. Catalysis and Mechanism of Malonyl Transferase Activity in Type II Fatty Acid Biosynthesis Acyl Carrier Proteins. *Mol. Biosyst.* **2009**, *5*, 651.
- (28) Wickramasinghe, S. R.; Inglis, K. A.; Urch, J. E.; Müller, S.; van Aalten, D. M. F.; Fairlamb, A. H. Kinetic, Inhibition and Structural Studies on 3-Oxoacyl-ACP Reductase from Plasmodium Falciparum, a Key Enzyme in Fatty Acid Biosynthesis. *Biochem. J.* **2006**, *393*, 447–457.
- (29) Fiers, W. D.; Dodge, G. J.; Sherman, D. H.; Smith, J. L.; Aldrich, C. C. Vinylogous Dehydration by a Polyketide Dehydratase Domain in Curacin Biosynthesis. *J. Am. Chem. Soc.* **2016**, *138*, 16024–16036.
- (30) Ward, W. H. J.; Holdgate, G. A.; Rowsell, S.; McLean, E. G.; Paupert, R. A.; Clayton, E.; Nichols, W. W.; Colls, J. G.; Minshull, C. A.; Jude, D. A.; Mistry, A.; Timms, D.; Camble, R.; Hales, N.J .; Britton, C. J.; Taylor, I. W. F. Kinetic and Structural Characteristics of the Inhibition of Enoyl (Acyl Carrier Protein) Reductase by Triclosan. *Biochemistry* **1999**, *38*, 12514–12525.

- (31) Xu, H.; Sullivan, T. J.; Sekiguchi, J. I.; Kirikae, T.; Ojima, I.; Stratton, C. F.; Mao, W.; Rock, F. L.; Alley, M. R. K.; Johnson, F.; Walker, S. G.; Tonge, P. J. Mechanism and Inhibition of SaFabI, the Enoyl Reductase from *Staphylococcus Aureus*. *Biochemistry* **2008**, *47*, 4228–4236.
- (32) Bonner, W. M.; Bloch, K. Purification and Properties of Fatty Acyl Thioesterase I from *Escherichia Coli*. *J. Biol. Chem.* **1972**, *247*, 3123–3133.
- (33) Salas, J. J.; Ohlrogge, J. B. Characterization of Substrate Specificity of Plant FatA and FatB Acyl-ACP Thioesterases. *Arch. Biochem. Biophys.* **2002**, *403*, 25–34.
- (34) Zhang, L.; Joshi, A. K.; Hofmann, J.; Schweizer, E.; Smith, S. Cloning, Expression, and Characterization of the Human Mitochondrial β -Ketoacyl Synthase: Complementation of the Yeast Cem1 Knock-out Strain. *J. Biol. Chem.* **2005**, *280*, 12422–12429.